J Appl Electrochem (2010) 40:1005–1018
DOI 10.1007/s10800-009-9974-3

ORIGINAL PAPER

Heterogeneous ion-selective membranes: the influence of the inert matrix polymer on the membrane properties

Karel Bouzek · Sabina Moravcová · Jan Schauer · Libuše Brožová · Zbyněk Pientka

Received: 29 October 2008 / Accepted: 18 August 2009 / Published online: 4 September 2009

Abstract Heterogeneous ion-exchange membranes were prepared by mixing small particles of sulfonated poly(1,4-phenylene sulfide) or sulfonated styrene–divinylbenzene copolymer with a matrix polymer. Four kinds of polymers were tested as a matrix: highly flexible linear polyethylene, medium-flexible fluoroelastomer, rigid polystyrene (all highly hydrophobic) and hydrophilic cellulose prepared by hydrolysis of cellulose acetate butyrate. Membrane morphologies were studied by scanning electron microscopy, IR spectroscopy and density measurements. Subsequently, the membranes were characterised with respect to their swelling in water, electrochemical characteristics and transport properties. Ion-exchange capacity and proton conductivity together with the permeability to hydrogen and methanol were investigated. The important impact of the ion-exchange particles as well as of the polymer matrix used was observed. The increasing rigidity of the polymer matrix resulted in a decrease in membrane permeability, but at the same time in deterioration of its ion-exchange capacity and subsequently of the proton conductivity, too. This was explained in terms of the limited elasticity of the polymer matrix, in each sample under study, which does not allow the ion-exchange particles to swell to an identical degree.

Keywords Ion-exchange membrane · Heterogeneous membrane · Ion-exchange capacity · Proton conductivity · Permeability

List of symbols

A	Membrane active area (m^2)
c	Molar concentration (mol m^{-3})
C	Ion-exchange capacity (mol kg^{-1})
D	Diffusion coefficient (m^2 s^{-1})
DS	Degree of swelling
e^0	Electron charge (C)
F	Faraday's constant (C mol^{-1})
j	Current density (A m^{-2})
k	Boltzmann constant (J K^{-1})
M	Partial molar volume of water (m^3 mol^{-1})
n	Molar amount (mol)
N	Number of water molecules absorbed per one ion-exchange group
N_{MeOH}	Number of methanol molecules transported by a proton
p	Pressure (Pa)
P	Permeability (m^2 s^{-1})
R	Universal gas constant (J mol^{-1} K^{-1})
T	Temperature (K)
V	Volume (m^3)
w	Weight (kg)
z	Charge number

Greek symbols

δ	Thickness (m)
ρ	Density (kg m^{-3})

K. Bouzek (✉) · S. Moravcová
Department of Inorganic Technology, Institute of Chemical Technology Prague, Technicka 5, 166 28 Prague 6, Czech Republic
e-mail: bouzekk@vscht.cz

J. Schauer · L. Brožová · Z. Pientka
Institute of Macromolecular Chemistry, Academy of Sciences of the Czech Republic, Heyrovsky Sq. 2, 162 06 Prague, Czech Republic

$\bar{\rho}$ Resistivity (Ω m)
τ Time (s)

Subscripts

calc	Calculated
d	Dry membrane
dif	Difference on the membrane
f	Feed compartment
H^+	Proton
H_2	Hydrogen
H_2O	Water
matrix	Matrix polymer
mem	Membrane
MeOH	Methanol
p	Product part of the permeation cell
powder	Ion-exchange powder
sw	Swollen membrane
v	vapour
vol	Voluminal

Superscripts

τ Time
0 Bulk concentration

1 Introduction

Ion-selective membranes are used as active separators in electrochemical processes, such as electrolysis or electrodialysis, and they are promising candidates for applications in proton exchange membrane fuel cells technology. Basically, they can be divided into two groups differing in their homogeneity: homogeneous membranes [1–4] visually appearing to consist of one phase and heterogeneous membranes containing micron-size ion-exchange particles embedded in an inert binder. An overwhelming majority of the so-far investigated membranes were homogeneous. Homogeneous membranes can exhibit excellent electrochemical properties, but this is most frequently at the expense of mechanical strength (except for extremely expensive perfluorinated membranes). On the other hand, heterogeneous membranes show very good mechanical properties but are somewhat less ion conductive.

Heterogeneous membranes can be prepared by:

(1) blending ion-exchange particles with a binder polymer and calendering, extruding or compression moulding the membrane from the blend [5, 6];
(2) suspending ion-exchange particles in a solution of an inert polymer, casting the membrane and evaporating the solvent [7–12];
(3) suspending ion-exchange particles in a solution of an inert polymer, casting the solution as a thin film and precipitating it in a nonsolvent bath [13, 14];
(4) dispersing ion-exchange particles in a liquid monomer or an uncured liquid polymer followed by polymerization in a mould [15].

Heterogeneous membranes based on an organic ion exchanger dispersed in a polyolefin were manufactured in Russia [16, 17] and, at present, in the Czech Republic (http://www.mega.cz). They are used mainly for electrodialytic separations in fairly aggressive environments. Although this fact is well known, the role of properties of the individual components in the ion selective membrane and the impact of their interactions on their material properties was not studied in detail. The aim of this article is to contribute to the understanding of this interesting class of materials.

The inert matrix plays evidently a decisive role in the long-term membrane stability. It protects the ion exchanger partly from the contact with the aggressive environment. At the same time, it has to allow a sufficiently intensive contact between the ion-exchanger particles, which provides a high ionic conductivity. Nor can be neglected the role of ion-exchange particles. Not only their transport properties, but also their size change with the degree of swelling and their interactions with the matrix polymer are important. Ion-exchanger particles made from derivatised styrene–divinylbenzene copolymers are commonly used as a functional material. This is because of their crosslinked structure imparting a high chemical stability to the material while keeping sufficient transport properties. Particles of other polymer materials, such as sulfonated poly(phenylene sulfide) [6, 13, 14] or of an inorganic ion-exchanger can be also used [18, 19, 20]. In our previous study [6, 21, 22] we sulfonated poly(phenylene sulfide) to various degrees to use the product as a functionalised membrane component. In this case, we were dealing with a noncrosslinked material with excellent transport properties. Sulfonated poly(phenylene sulfide), if functionalised to a very high degree, is characterised by an extremely high water uptake (in contrast to crosslinked styrene–divinylbenzene copolymers). The aim of this study was to prepare heterogenous membranes based on various matrix polymers (differing in structure and mechanical properties) with the two above ion-exchange materials and to investigate the influence of the components on the properties of resulting membrane, mainly with respect to its future utilisation in the direct methanol fuel cell.

2 Experimental

2.1 Materials

Poly(1,4-phenylene sulfide) (PPS) (Aldrich, nominal M_n ca. 10,000, powder), sulfuric acid fuming (Aldrich, ACS reagent, SO_3 content 17%), sulfuric acid 98% (Fluka), linear

polyethylene (ExxonMobil, EXACT^{TM} 0210), polystyrene (Krasten 171, Kaucuk Kralupy, Czech Republic), poly(vinylidene fluoride-*co*-hexafluoropropylene) (fluoroelastomer) (Aldrich, nominal $M_w = 400{,}000$) and cellulose acetate butyrate (Aldrich, nominal $M_n = 65{,}000$, 29.5 wt% of acetyl and 17 wt% of butyryl content) were used as received. Amberlite 252 Na (sulfonated polystyrene ion-exchanger) (Rohm and Haas) with predominant particle size of 10–25 μm was obtained from MEGA Co. (Czech Republic).

2.2 Preparation of sulfonated PPS

PPS powder (50 g) was mixed with sulfuric acid (184 g), and then fuming sulfuric acid (320 g) was slowly added. The mixture was stirred at room temperature until it changed to a gel (ca. 1 h). It was left standing for 16 h in dry atmosphere, then diluted and washed with icy water, treated with aqueous 1 M sodium hydroxide to transfer it into the Na^+ form (16 h) and washed thoroughly with water (several days) and dried at 90 °C. The dried product was ground in a ball mill and sieved (50 μm mesh) to obtain small particles. For its structural formula, see Fig. 1. The particle size was relatively large for several applications, such as fuel cell technology, but it was satisfactorily for the present purpose. The degree of PPS sulfonation 43.7% was calculated from the Na content in the polymer in this ion cycle (6.58%) determined by the elemental analysis.

2.3 Membrane preparation

Sulfonated PPS or Amberlite particles were blended with a matrix polymer (34 wt%) in a Brabender Plasti-corder PLE 651 at a temperature above the melting point of the matrix polymer until the mixture became optically homogeneous and the torque value reached constant value. The concentration of ion-exchange particles in the membrane was kept constant at 66 wt% (dry weight) as it was found in the previous study (with polyethylene matrix) that such membranes possess the required mechanical strength and ionic conductivity [6, 21]. The blends were press-moulded between two poly(ethylene terephthalate) films (all blends except cellulose acetate butyrate ones) or aluminium foils (cellulose acetate butyrate) at 10 MPa. The temperature in the Brabender chamber and of the press plates was 150 °C (linear polyethylene), 190 °C (polystyrene blends), 220 °C (fluoroelastomer blends) or 230 °C (cellulose acetate butyrate). The resulting (flat) membrane was typically 0.25 mm thick. Membranes containing cellulose acetate butyrate matrix were immersed then in excess of 2% aqueous NaOH (12 h) to hydrolyse the matrix polymer to (regenerated) cellulose and washed in deionised water.

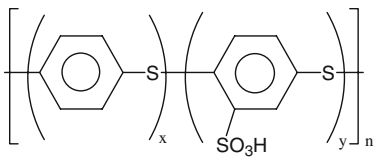

Fig. 1 Sulfonated poly(1,4-phenylene sulfide)

Prior to testing, each membrane was activated by the following procedure:

- Swelling in the demineralised water
- Diving for 12 h in excess of 1 M HCl
- Diving for 12 h in excess of 1 M NaOH
- Diving for 12 h in excess of 1 M HCl
- Diving for 12 h in demineralised water

During the membrane transfer from HCl to NaOH and in the opposite direction, it was washed in demineralised water. Subsequently, the membrane was ready for the testing.

2.4 Tensile strength testing

Tensile strength testing of sheets prepared from unfilled matrix polymers was carried out with an Instron 5800 R testing machine at room temperature. The test specimens were 5 cm in length and 1 cm wide. Modulus of elasticity was determined at the cross-head speed 1 mm min^{-1} up to 1% strain, tensile break stress and strain at the cross-head speed 20 mm min^{-1}. The reported results are mean values of five replicates.

2.5 Microscopy

The morphology of the prepared membranes was investigated using a Hitachi scanning electron microscope S4700. Membranes dried in dessicator over molecular sieves were immersed into liquid nitrogen, broken, placed in a metal holder and coated with a gold/palladium layer by sputtering under vacuum.

2.6 Spectroscopy

The FTIR-ATR spectra were measured using a Perkin-Elmer 1000 PC spectrometer with the MKII GG SR ATR system (diamond/45 °C), resolution 4 cm^{-1}, 16 scans. The powdery samples were pressed together with KBr into pellets (2 mg sample/350 mg KBr). A sample of the membrane bulk was prepared by freezing in the liquid nitrogen and grinding in a ball mill.

2.7 Density

Densities of membranes, sulfonated PPS and Amberlite powders and matrix polymers were determined with helium pycnometer (Picnomatic, Porotec) at 20 °C. Membrane densities were also calculated using Eq. 1

$$\rho_{\text{calc}} = 0.34\rho_{\text{matrix}} + 0.66\rho_{\text{powder}} \quad (1)$$

where ρ_{matrix} and ρ_{powder} are the densities of the matrix polymer and the ion-exchange powder, respectively.

2.8 Degree of swelling

The sorption of water in membranes was determined using a laboratory high vacuum apparatus consisting of a vacuum balance (Sartorius 4102), diffusion vacuum pump (Balzers), dosing valve, water vapour reservoir and pressure transducer (BD Sensors DMP331). Samples of the membranes, placed in the balance, were first thoroughly dried for 8 h at 40 °C under vacuum. Then, the apparatus was filled with water vapour at the desired pressure. The degree of swelling (DS) was evaluated from the increase in the weight of the sample according to Eq. 2.

$$\text{DS} = \frac{w_{\text{sw}} - w_{\text{d}}}{w_{\text{d}}} \quad (2)$$

where w_{sw} and w_{d} are the weights of the swollen and the dry membrane, respectively.

The change in the sample volume related to the swelling by the water vapour (volumetric degree of swelling) of Amberlite and sulfonated PPS powders was obtained by determining the volumes of dry powders and powders swollen for 48 h in water, respectively, in a cylinder and calculated using Eq. 3,

$$\text{DS}_{\text{vol}} = \frac{V_{\text{sw}} - V_{\text{d}}}{V_{\text{d}}} \quad (3)$$

where V_{sw} and V_{d} are the volumes of the swollen and the dry powders, respectively.

2.9 Ion-exchange capacity

The ion-exchange capacity of the free ion-exchanger particles as well as the synthesised membranes was determined. A combined glass electrode was left to equilibrate with a 0.1 M NaCl solution. Afterwards, a conditioned powder or membrane in the H^+ form was plunged into the continuously agitated solution. The time response of the glass electrode potential was recorded. With the use of the calibration curve, the amount of H^+ ions disengaged from the membrane was estimated.

A Ross combined glass electrode (Orion) was used during this series of experiments. A Keithley 6514 electrometer with an input impedance of 200 TΩ was used to read a glass electrode signal. This arrangement provides sufficient glass electrode signal stability and reproducible results.

2.10 Determination of proton conductivity

The conductivity of the membrane was measured in a longitudinal direction in a tempered box under nitrogen atmosphere at dew point (relative humidity 100%), Testo 635 humidity meter was used. Electrochemical impedance spectra (EIS) of the membrane were measured in the four-electrode arrangement. A Frequency Response Analyser Solartron SI 1250 in connection with an Electrochemical Interface Solartron SI 1287 was used for this purpose.

2.11 Determination of proton diffusion coefficients

The proton diffusion coefficient in the membrane D_{H^+} was evaluated from the membrane conductivity using a theory developed by Millet [23]. This theory is based on the Einstein relationship between absolute ionic mobility and diffusion coefficient, which considers the membrane as a homogeneous continuum. The diffusivity value evaluated is thus valid for a pseudohomogeneous membrane. If a single univalent counter ion is present in the membrane interior, then its diffusion coefficient can be evaluated according to the Millet theory from the membrane conductivity or the membrane resistivity measured by the means of the following relationship:

$$D_{H^+} = \frac{kT}{z_{H^+}^2 \bar{\rho}_{\text{mem}} c_{\text{mem},H^+} \text{Fe}^0} \quad (4)$$

where $\bar{\rho}_{\text{mem}}$ is the membrane resistivity (inverse of the conductivity), k the Boltzmann constant, T the temperature, e^0 electron charge, F the Faraday's constant and c_{mem,H^+} the mobile ion concentration in the membrane, z_{H^+} the proton charge number,

$$c_{\text{mem},H^+} = \frac{\rho_{\text{mem}} C}{1 + \rho_{\text{mem}} N_{H_2O} M_{H_2O} C} \quad (5)$$

where ρ_{mem} is the density of the dry membrane, N_{H_2O} the water to ion-exchange site mole ratio, M_{H_2O} the water partial molar volume and C the ion-exchange capacity.

2.12 Permeability to hydrogen

The gas transport properties of the membranes were determined using a laboratory high-vacuum apparatus with a static permeation cell shown in Fig. 2. At the beginning, both parts of the cell—feed and product—were filled with water vapour under the required pressure p_{f,H_2O} to swell the membrane until equilibrium was attained. The permeation

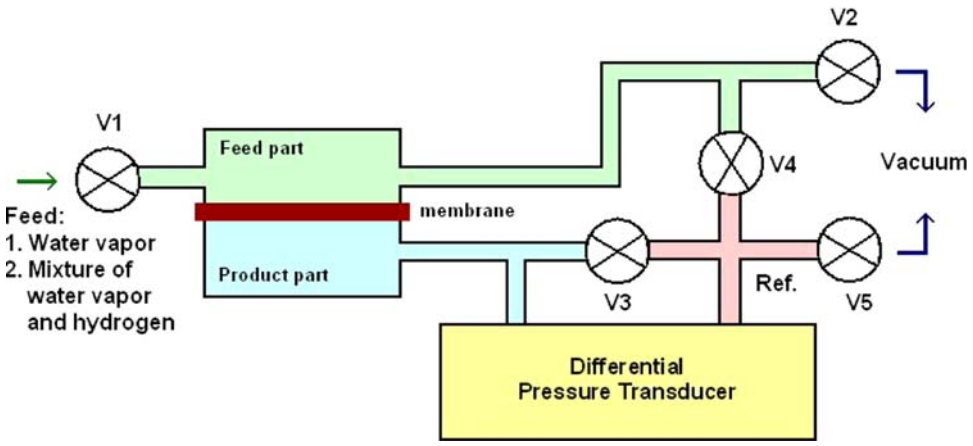

Fig. 2 Apparatus for determination of the membrane permeability to hydrogen. At the beginning, both parts of the permeation cell are fed with water vapour: valves V1, V3,V4 are open. After the equilibrium is attained, valves V3 and V4 are closed. During hydrogen permeation only V1 is open

experiment started when the mixture of hydrogen under constant pressure p_{f,H_2} (120 kPa) and water vapour under pressure p_v was brought into the feed. Hydrogen passed through the membrane under the driving force of its partial pressure difference, which is virtually equal to p_{dif,H_2}, hence the pressure p_{p,H_2}, in the product side increased. The permeability P was determined from the slope of the increase in the pressure p_{p,H_2}, in the calibrated volume V_p of the product part of the cell in time during the permeation experiment $\left(\frac{dp_{p,H_2}}{d\tau}\right)$. Permeability was calculated using the formula

$$P_{H_2} = \frac{dp_{p,H_2}}{d\tau}\frac{V_p\delta_{mem}}{Ap_{dif,H_2}}\frac{1}{RT} \quad (6)$$

where δ_{mem} is membrane thickness, A its active area, T temperature and R the universal gas constant. All the measurements were carried out at 30 °C. For each type of membrane, the measurement was repeated at least four times with different samples. The permeabilities reported here are the mean values in the case of polyethylene- and fluoroelastomer-based membranes. In the case of the polystyrene-based membranes, the lowest determined permeability value was used.

2.13 Permeability to methanol

The cell used to determine membrane permeability for methanol is schematically shown for the currentless conditions in Fig. 3a and for the membrane under current load in Fig. 3b. The cell consists of two compartments made of glass separated by the membrane under study.

In the case of the membrane under currentless conditions, at the start of the experiment the permeate compartment is filled with demineralised water and the feed compartment with 1 M MeOH solution in demineralised water. Samples are taken at defined time intervals from the permeate side of the membrane. The content of the

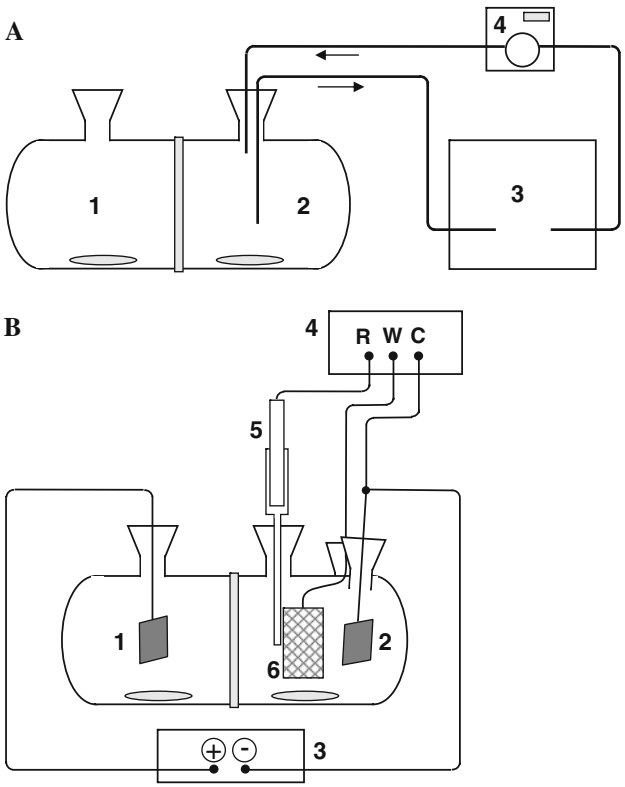

Fig. 3 Apparatus for determination of the membrane permeability to methanol under **a** currentless conditions: 1—reservoir with MeOH solution, 2—permeate reservoir, 3—refractometer and 4—pump; **b** current load: 1—reservoir with MeOH solution, 2—permeate reservoir, 3—stabilised power source, 4—potentiostat, 5—reference electrode and 6—Pt mesh electrode

methanol is determined using a Knauer 2025/50 differential refractometer by means of a calibration curve.

In the case of the membrane current load, the permeate compartment is filled with 0.5 M H_2SO_4 solution in demineralised water. The feed compartment then contains a 1 M MeOH solution in 0.5 M H_2SO_4. This supporting electrolyte is used to simulate a PEM fuel cell environment.

Both compartments are equipped with a Pt foil electrode used to impose the defined current load on the membrane. The permeate compartment contains an additional Pt mesh electrode and a saturated argent chloride electrode allowing determination of the amount of penetrated methanol by cyclic voltammetry [24].

For a single layer separator an expression for the variation of the molar amount of methanol in the permeate compartment originally containing demineralised water only may be described as follows

$$\frac{\mathrm{d}n^{\tau}_{\mathrm{p,MeOH}}}{\mathrm{d}\tau} = P_{\mathrm{MeOH}}\frac{c^{\tau}_{\mathrm{f,MeOH}} - c^{\tau}_{\mathrm{p,MeOH}}}{\delta_{\mathrm{mem}}}A, \tag{7}$$

where P_{MeOH} indicates membrane permeability to methanol. The concentrations of methanol in the two compartments are interconnected by a molar balance.

$$c^{\tau}_{\mathrm{f,MeOH}}V_{\mathrm{f}} = c^{\tau=0}_{\mathrm{f,MeOH}}V_{\mathrm{f}} - c^{\tau}_{\mathrm{p,MeOH}}V_{\mathrm{p}} \tag{8}$$

By integrating Eq. 8 into Eq. 7, after a simple rearrangement the resulting equation may be integrated into the time interval 0 s to τ. An expression for the content of methanol in the permeate compartment in dependence on time is obtained.

$$n^{\tau}_{\mathrm{p,MeOH}} = \frac{V_{\mathrm{p}}c^{\tau=0}_{\mathrm{f,MeOH}}}{\frac{V_{\mathrm{p}}}{V_{\mathrm{f}}}+1}\left\{1 - \exp\left[-\frac{P_{\mathrm{MeOH}}A}{\delta_{\mathrm{mem}}V_{\mathrm{p}}}\left(\frac{V_{\mathrm{p}}}{V_{\mathrm{f}}}+1\right)\tau\right]\right\} \tag{9}$$

After rearranging Eq. 9, an expression for P_{MeOH} in the form of Eq. 10 can be obtained.

$$P_{\mathrm{MeOH}} = -\frac{\delta_{\mathrm{mem}}V_{\mathrm{p}}}{A\left(\frac{V_{\mathrm{p}}}{V_{\mathrm{f}}}+1\right)\tau}\ln\left[1 - \frac{n^{\tau}_{\mathrm{p,MeOH}}\left(\frac{V_{\mathrm{p}}}{V_{\mathrm{f}}}+1\right)}{V_{\mathrm{p}}c^{\tau=0}_{\mathrm{f,MeOH}}}\right] \tag{10}$$

In the case of the membrane under current load the number of the methanol molecules being transported in a solvatation shell of a proton can be evaluated by means of Faraday's law. It is based on the known current load used and the self-diffusion rate.

$$N_{\mathrm{MeOH}} = \frac{F}{j}\left[\frac{V_{\mathrm{p}}}{A}\frac{\mathrm{d}c^{\tau}_{\mathrm{p,MeOH}}}{\mathrm{d}\tau} - P_{\mathrm{MeOH}}\frac{\left(c^{\tau}_{\mathrm{f,MeOH}} - c^{\tau}_{\mathrm{p,MeOH}}\right)}{\delta_{\mathrm{mem}}}\right] \tag{11}$$

By using the material balance given by Eq. 8, after separation of variables and integration Eq. 11 takes the following form.

$$N_{\mathrm{MeOH}} = \frac{F}{j}\left\{\frac{V_{\mathrm{p}}}{A}\frac{c^{\tau}_{\mathrm{p,MeOH}}}{\tau} + \frac{P_{\mathrm{MeOH}}}{\delta_{\mathrm{mem}}} \times \left[\frac{V_{\mathrm{f}}}{V_{\mathrm{p}}}c^{\tau=0}_{\mathrm{f,MeOH}} - \left(1+\frac{V_{\mathrm{f}}}{V_{\mathrm{p}}}\right)c^{\tau}_{\mathrm{p,MeOH}}\right]\right\} \tag{12}$$

3 Results and discussion

3.1 Membrane preparation and structure

3.1.1 Membrane preparation

Four kinds of polymers were tested as matrixes in heterogeneous membranes: highly flexible linear polyethylene, medium flexible fluoroelastomer, rigid polystyrene (all highly hydrophobic) and cellulose acetate butyrate. The last mentioned material, after incorporation into a heterogeneous membrane, was converted by the treatment with aqueous sodium hydroxide to hydrophilic cellulose. Tensile properties of the neat matrix polymers used are listed in Table 1.

Two kinds of ion-exchange particles were incorporated into heterogeneous membranes—Amberlite and sulfonated PPS. The particles differ slightly in their ion-exchange capacity, but the main difference consists in their structure. While Amberlite has a crosslinked structure, sulfonated PPS is a noncrosslinked material. Therefore, these materials have generally different swellabilities when exposed to water.

While there were no problems in the preparation of membranes containing linear polyethylene, some force had to be exerted to detach the membranes containing polystyrene or fluoroelastomer matrix from poly(ethylene terephthalate) films used as separators in moulding. This resulted in some cases in the formation of small cracks in membranes as manifested by their increased permeability discussed later on.

This behavior was connected with the mechanical properties of the membranes prepared. Modulus of elasticity increased and break strain of heterogeneous membranes decreased with the increasing content of particles in the heterogeneous membrane structure (the membrane elasticity was deteriorated). This continues up to the particle concentration of 66 wt%. Above this level, the membranes

Table 1 Tensile properties and water sorption of neat matrix polymers

Matrix polymer	Modulus of elasticity (MPa)	Break stress (MPa)	Break strain (%)	Water sorption (%)
Linear polyethylene	3	22	770	<0.01
Fluoroelastomer	736	48	460	<0.01
Polystyrene	3,100	42	1.4	<0.1
Water-swollen cellulose[a]	120	7.7	13	37

[a] Obtained by hydrolysis of cellulose acetate butyrate

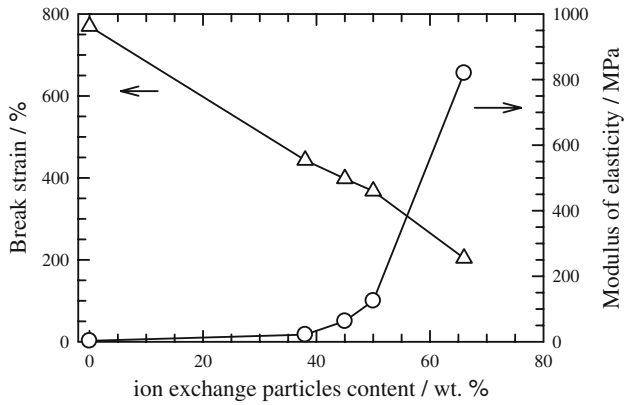

Fig. 4 Dependence of the heterogeneous membrane's mechanical properties on the content of the polymer exchange particles in the matrix polymers, sulfonated PPS particles in linear polyethylene: *open circle* modulus of elasticity and *open triangle* membrane break strain, temperature 22 °C

lose their mechanical strength as not all ion-exchange particles are properly bonded in the polymer matrix. This is documented for the case of linear polyethylene and sulfonated PPS particles in Fig. 4. The remaining matrix polymers show qualitatively the same dependences (with an exception of the cellulose acetate butyrate matrix, as discussed later in the text) and therefore are not shown here. The values of the modulus of elasticity obtained for the individual membranes are shown in Table 3. As it can be seen, at the conditions of the experimental nature of the ion-exchange particles does not have a significant influence on this parameter. Important is just their content.

After conversion to hydrophilic cellulose, the membranes with the cellulose acetate butyrate matrix showed extremely poor mechanical strength and were difficult to handle. Therefore, they were excluded from the detailed characterisation.

3.1.2 Membrane morphology

SEM was used to provide primary characterisation of the prepared membranes morphology. Micrographs of typical Amberlite membrane cross-sections are shown in Fig. 5a–d. Whereas Amberlite particles in the cellulose matrix shown in Fig. 5a appear to be tightly surrounded by the inert polymer with only minimum contacts between the particles, the polyethylene matrix shown in Fig. 5b exhibits significantly more promising properties. Its structure is porous, and thus the ion transport can proceed either by a direct contact of ion-exchanger particles or by short channels filled up with the electrolyte. The structure of a fluoroelastomer-based membrane shown in Fig. 5c is similar to that of a polyethylene-based one, only the matrix of the former polymer is more rigid. The membranes with a polystyrene matrix are, on the contrary, dense. As can be seen in Fig. 5d, individual particles are tightly surrounded by the polymer matrix, and their interconnections are strongly limited.

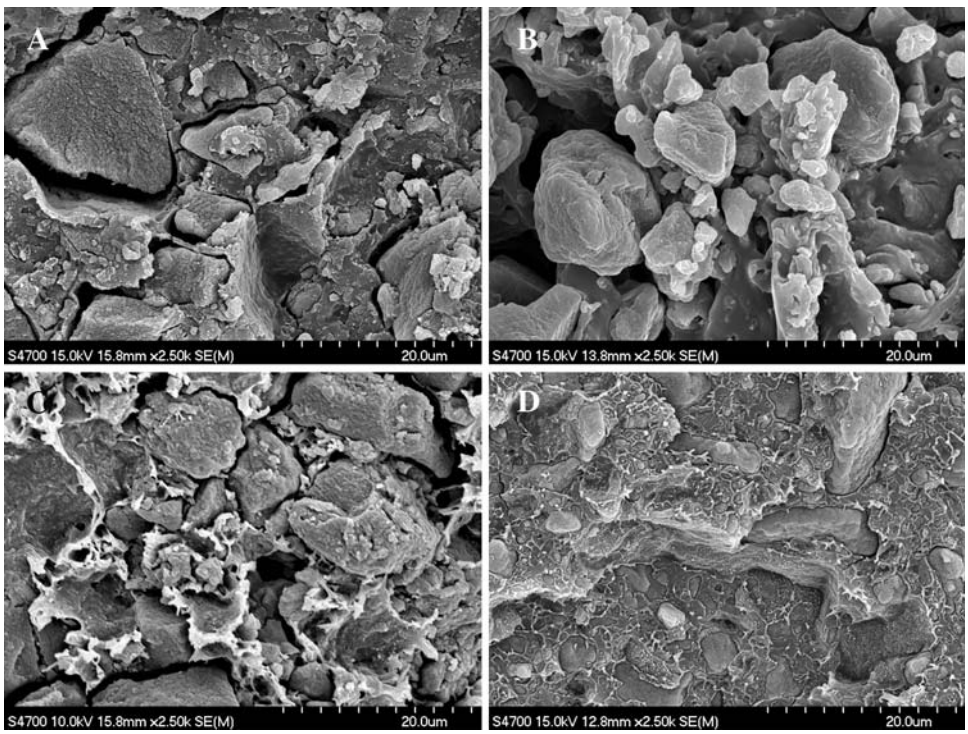

Fig. 5 SEM micrographs of cross-sections of heterogeneous Amberlite membranes based on **a** cellulose, **b** polyethylene, **c** fluoroelastomer and **d** polystyrene matrix

The reason consists in different elasticities of polymers. The modulus of elasticity values of the fluoroelastomer is by more than two orders of magnitude higher and that of polystyrene by three orders of magnitude higher than that of polyethylene. Elastic polyethylene matrix (and less the fluoroelastomer matrix) accommodates to a certain extent larger ionomer particles due to the humidity of the membrane environment. SEM microphotographs were taken in a high vacuum; hence the particles are dry and contracted again, and the cavities between the matrix and the particles may be formed. The existence of the cavities additionally indicates that polyethylene and fluoroelastomer do not interact significantly with the ionomer.

The above results indicate that polyethylene shows the most promising properties as a matrix polymer. Figure 6 shows a comparison of structures of membranes based on Amberlite and sulfonated PPS particles bound by a polyethylene matrix. The membrane carrying Amberlite particles has a higher number of pores of lower diameter, which indicates better interconnection of the particles and which promotes high membrane conductivity and permeability. This may primarily result from smaller sizes of Amberlite particles. It is, however, important to keep in mind that the matrix polymer properties determine only partly properties of the whole membrane.

The mould-pressing is carried out at temperatures above the melting points of matrix polymers. Under these conditions, the ion-exchanger particles are surrounded by the film of a matrix polymer, and the membrane surface is formed preferably by this polymer. The surface layers (skin) of polyethylene—Amberlite and polyethylene—sulfonated PPS membrane are shown in Fig. 7a and b. The micrographs indicate that the polyethylene—sulfonated PPS membrane has a skin more compact and thicker than the polyethylene—Amberlite one. The difference between the two membranes consists also in the number of surface defects exposing the ion-exchange particle at the surface. They seem to be more frequent in the case of the Amberlite ionomer.

The presence of skin is confirmed also by IR spectroscopy. Figure 8 compares the spectra of the sheet surface comprising only linear polyethylene (curve A), the surface of the heterogeneous membrane of linear polyethylene and sulfonated PPS (B); the bulk of the same membrane (C) and the spectra of sulfonated PPS powder (D). The surface of the heterogeneous membrane is very similar to that of pure linear polyethylene except for medium strong signals of the sulfonic acid group at 1,059 cm^{-1} (ν_s S=O) and 1,195 cm^{-1} (ν_{as} S=O), and a very weak band at about 860 cm^{-1} (out-of-plane CH deformation vibration of 1,2,4-trisubstituted benzene ring in sulfonated PPS). The spectra of the bulk of the membrane (obtained by freezing the membrane in liquid nitrogen and grinding it in a ball mill) resembles, on the contrary, that of pure sulfonated PPS

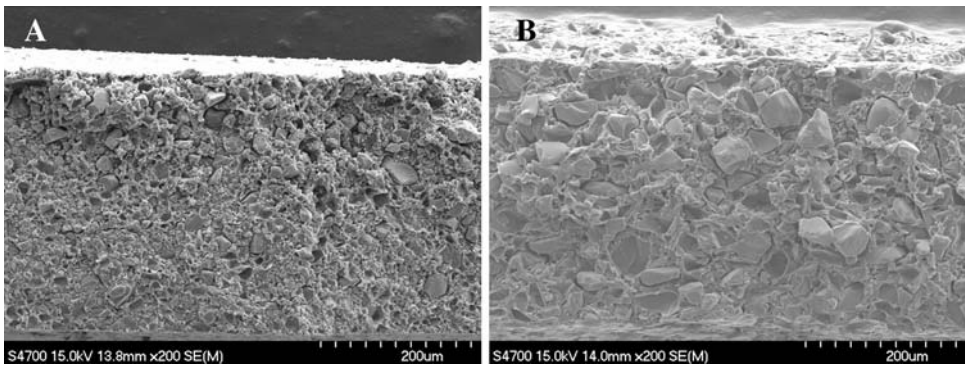

Fig. 6 SEM micrographs of cross-sections of heterogeneous membranes: **a** linear polyethylene—Amberlite, **b** linear polyethylene—sulfonated PPS

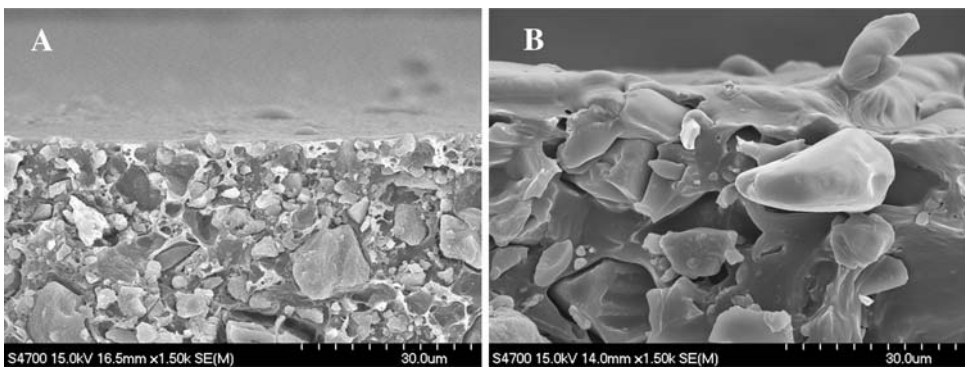

Fig. 7 SEM micrographs of the surface region (skin) of heterogeneous membranes: **a** linear polyethylene—Amberlite, **b** linear polyethylene—sulfonated PPS

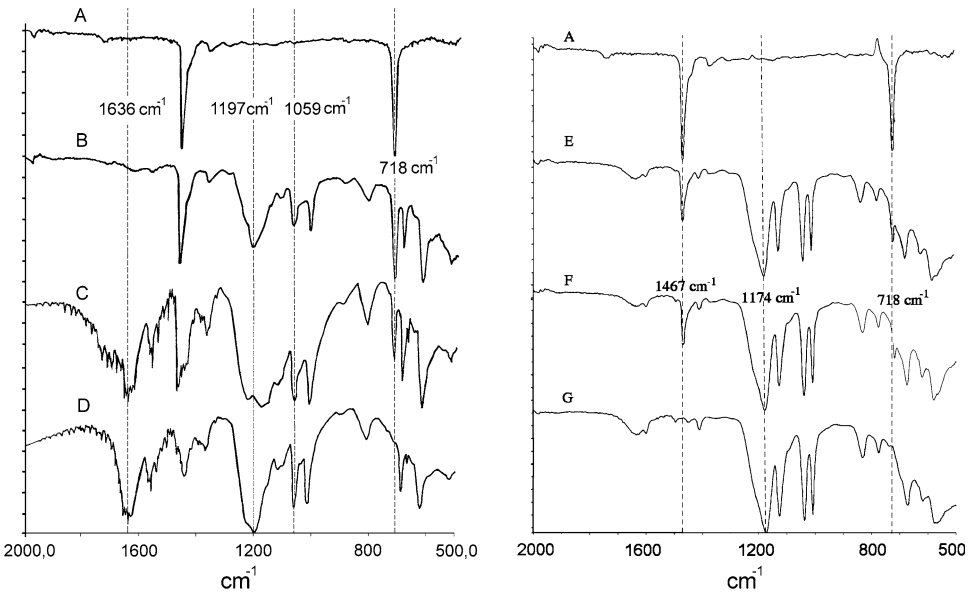

Fig. 8 IR spectra of the membranes: (A) surface of neat linear polyethylene; (B) surface of the heterogeneous membrane linear polyethylene—sulfonated PPS; (C) bulk of the heterogeneous membrane linear polyethylene—sulfonated PPS; (D) sulfonated PPS powder; (E) surface of the heterogeneous membrane linear polyethylene—Amberlite; (F) bulk of the heterogeneous membrane linear polyethylene—Amberlite; (G) Amberlite powder

particles. Note that the membrane was prepared by blending 66 wt% of sulfonated PPS particles and only 34 wt% of linear polyethylene.

The same experiment was performed with Amberlite embedded in polyethylene. Its results are summarised in Fig. 8 as well. As it can be seen, the spectra of the surface of the heterogeneous membrane (E) do not show any significant difference from those of the bulk of the membrane (F). In both of them, a significant signal of the Amberlite particles is clearly visible (G). This means that the thickness of the skin film on the surface of this particular membrane is smaller than 1 μm, which is in good agreement with the observation made by SEM (Fig. 7a).

An attempt was made to determine the skin film thickness quantitatively for the individual membrane materials under study by the means of SEM pictures. Unfortunately, it was not successful due to the significant inhomogeneity of the skin layer thickness across the membrane surface.

Closer analysis of the morphology of the samples prepared has confirmed the importance of the skin layer. Although this layer may have a negative effect on the ionic conductivity of the membrane, an important point is that the skin formed predominantly by a matrix polymer improves mechanical properties of the membrane and protects the ion-exchanger particles against an intensive attack by aggressive environment.

3.1.3 *Membrane porosity*

Another important aspect, in which heterogeneous membranes differ from homogeneous ones, consists in the existence of cavities in the bulk of the membrane. Whereas in homogeneous membranes such cavities may be formed only as a result of fast solvent evaporation, in the case of heterogeneous membranes they may result from different thermal expansivity of the matrix polymer and ion-exchanger particles. In this study, the density values determined with the helium pycnometer were compared with those calculated as a linear combination of the densities of a neat ion exchanger and a matrix polymer (see Eq. 1 and Table 2). The results

Table 2 Membrane densities measured and calculated and their ratio

Ion-exchange polymer	Matrix polymer	ρ_m [a] (g cm^{-3})	ρ_{calc} [b] (g cm^{-3})	ρ_m/ρ_{calc} (%)
Amberlite	Linear polyethylene	1.13	1.26	90
Amberlite	Fluoroelastomer	1.44	1.56	93
Amberlite	Polystyrene	1.20	1.31	92
Sulfonated PPS	Linear polyethylene	1.16	1.36	85
Sulfonated PPS	Fluoroelastomer	1.54	1.66	93
Sulfonated PPS	Polystyrene	1.23	1.41	87

[a] Membrane density measured

[b] Membrane density calculated using Eq. 1. Densities of components: Amberlite powder 1.44 g cm^{-3}, sulfonated PPS powder 1.60 g cm^{-3}, linear polyethylene 0.90 g cm^{-3}, fluoroelastomer 1.78 g cm^{-3}, polystyrene 1.05 g cm^{-3}

obtained clearly indicate the cavity formation. The membranes containing sulfonated PPS show higher volume of cavities than those based on Amberlite. This can be explained by the size of the sulfonated PPS particles, which is more than double of that of Amberlite and by their significantly higher swellability in humid atmosphere. However, the influence of the matrix polymer on the membrane porosity was not detected. In this case, it is because of the limited reproducibility of the membrane preparation.

3.2 Membrane physico-chemical properties

The membranes prepared and characterised in terms of their structure and morphology in the preceding part of this study were characterised to obtain further details on their properties and a more profound understanding of the nature of the interaction between the polymer matrix and the ion-exchange particles and their impact on the resulting membrane properties. The membranes based on the cellulose acetate butyrate binder did not show sufficient mechanical properties and thus their electrochemical and transport properties could not be conclusively determined.

3.2.1 Degree of the membrane swelling

The degree of membrane swelling represents an important parameter which has a significant impact on the conductivity and permeability of the membrane and also on its mechanical strength. It characterises the degree of the openness and flexibility of the membrane structure as well as the concentration of the hydrophilic ion-exchange sites. Therefore, it was determined in the present case.

In the first instance, the stand-alone ion-exchange particles were tested. At a temperature of 20 °C and relative atmosphere humidity of 100%, Amberlite particles take up 47 wt% of water. This is connected with an increase in their volume of 80%. By contrast, under identical conditions sulfonated PPS particles absorb 82 wt% of water, which increases its volume by 1,500%.

This result corresponds well to the membrane swelling determined, which is summarised in Table 3. As expected, Amberlite-based membranes show practically no influence of the matrix polymer elasticity on their degree of swelling at 100% relative humidity. This is connected with the fact that the changes in the dimensions of these ion-exchanger particles, induced by the swelling by the water vapour, are relatively low and can thus be accommodated by the matrix polymer. It is interesting to note that, in the case of the Amberlite-based membranes, the amount of adsorbed water exceeds the amount corresponding to the content of 66 wt% of the ion-exchange resin in the membrane, i.e. 31 wt%. This is due to the condensation of the water in the cavities and pores of the heterogeneous membrane.

Sulfonated PPS, on the other hand, expands significantly more under the conditions under investigation. Linear polyethylene is still able to accommodate such a change to a certain degree. This is, however, not the case with the remaining two polymers. They can only accommodate sulfonated PPS particle expansion to a strictly limited extent. Therefore, the amount of adsorbed water decreases significantly with the decreasing elasticity of the matrix polymer and again reaches a value of nearly 50 wt% as in the case of the rigid Amberlite particles. This value is comparable, or slightly lower when compared to the sulfonated PPS by itself. It can be assumed that, in this case, the amount of water condensed in the free volume between the ion-exchange particles and the matrix phase is negligible.

3.2.2 Ion-exchange capacity

In the first step, the ion-exchange capacity of free ion-exchange particles was determined with the aim of obtaining a reference point. In the case of the Amberlite powder, an ion-exchange capacity of 8.2 mmol g^{-1} of a dry material was determined. The sulfonated PPS showed an ion-exchange capacity of 35.1 mmol g^{-1} of a dry polymer. As shown in Table 3, if incorporated into the polymer matrix, then the ion-exchange capacity of the material is reduced due to the addition of an inert matrix phase. Since the amount of dry ion exchanger in the heterogeneous membrane is kept constant at 66 wt%, the ion-exchange capacity of the sample should reach a value of 5.4 and 23.2 mmol g^{-1} for the Amberlite and sulfonated PPS-based membranes, respectively. The difference is clearly caused by the limited elasticity of the polymer matrix. Since the membranes are press-moulded, the ion-exchanger particles are present after synthesis in the matrix in the dry, unexpanded form. Dissociation of the ion-exchange groups of the particles is connected with the sorption of the substantial amount of water, and thus with the increase in particle volume. The reduced elasticity of the polymer matrix phase results in their limited expansion and thus also, to a certain degree, in the limited accessibility of the ion-exchange phase. This theory is supported by the fact that in the case of the cross-linked Amberlite this effect is not very significant. That is because the structure of this ion-exchange resin is relatively rigid and it is not subject to significant volume changes during the swelling. On the contrary, the swelling of the sulfonated PPS is connected with important volume changes that cannot be accommodated by the polymer matrix. An additional important factor is the size of the ion-exchange particles. In the case of the sulfonated PPS the average particle diameter is two to three times larger than the Amberlite particles. This results in the larger local volume changes related to the one sulfonated PPS particle when compared to the Amberlite. At the same time, the surface-to-

Table 3 Membrane characteristics determined for the individual combinations of the ion-exchanger particles and matrix polymers

Ion exchanger	Matrix polymer	DS[a] (wt%)	IEC[b] (mmol g^{-1})	Conductivity 35[c] (S m^{-1})	Conductivity 60[c] (S m^{-1})	$D_H \times 10^{10}$[d] (m^2 s^{-1})	$P_{MeOH} \times 10^{11}$[e] (m^2 s^{-1})	P_{MeOH} (j) $\times 10^{11}$[f] (m^2 s^{-1})	N[g]	$P_{H_2} \times 10^{15}$[h] (mol m^{-1} s^{-1} Pa^{-1})	G[i] (MPa)
Amberlite	Linear polyethylene	50	3.25	4.17	6.36	4.69	8.8	25.2	0.18	3.6	880
Amberlite	Fluoroelastomer	52	2.94	3.42	4.72	4.32	NA	NA	NA	1.9	4200
Amberlite	Polystyrene	51	2.77	1.70	1.93	2.27	1.9	12.1	0.06	NA	>10000
Sulfonated PPS	Linear polyethylene	70	1.75	3.87	9.59	9.28	12.4	41.6	0.32	2.6	820
Sulfonated PPS	Fluoroelastomer	49	1.98	3.50	4.78	6.45	7.6	17.7	0.06	1.5	3900
Sulfonated PPS	Polystyrene	47	1.70	2.36	3.25	4.99	1.9	13.9	0.09	NA	>10000
Nafion 117		39	0.99[j]	7.80[j]		3.5[j]	9.9	44.7	0.53	5.4	232

[a] Degree of swelling at 100% relative humidity

[b] Proton ion-exchange capacity related to the weight of the dry membrane in the proton cycle

[c] Conductivity of the membrane in the proton cycle at 35 and 60 °C and 100% relative humidity

[d] Proton diffusion coefficient in the membrane in the proton cycle at 100% relative humidity at 35 °C

[e] Permeability of the membrane in the proton cycle to the methanol at 22 °C

[f] Permeability of the membrane in the proton cycle to the methanol at 22 °C under current load of 25 mA cm^{-2}

[g] Number of methanol molecules transported through the membrane by the proton migrating through the membrane under current load at 22 °C

[h] Permeability of the membrane to the hydrogen at 20% relative humidity and 25 °C

[i] Modulus of elasticity at 22 °C

[j] At the temperature of 20 °C

volume ratio is less favourable for rapid and efficient mass exchange. Thus, sulfonated PPS-based membranes are more significantly influenced by the mechanical properties of the matrix polymer.

3.2.3 *The influence of the matrix polymer and properties of the ion-exchange particles on heterogeneous membrane conductivity*

The dependency of the proton conductivity of the prepared membrane samples on the modulus of elasticity of matrix polymers is shown in Fig. 9 for both ion-exchanger particles used during this study. The related results are summarised in Table 3. Two phenomena may be observed with respect to this dependence. The first one clearly consists in the significantly decreasing membrane conductivity with the increasing value of the elasticity modulus. Here, an explanation similar to the ion-exchange capacity and water swelling applies. The limited elasticity or even rigidity of the matrix polymer strongly limits the swelling of the particles. Proton transport pathways, therefore, have not developed to a sufficient extent. As a consequence, the membrane conductivity decreases.

The second phenomenon consists in the development of the membrane conductivity with the temperature. At 35 °C, the conductivity of the membranes shows more or less identical values for both types of ion-exchange resins. This clearly documents the decisive role of the polymer matrix. At 60°, the conductivity of the membranes based on the sulfonated PPS systematically exceeds the conductivity of the membranes containing Amberlite. This is especially pronounced in the membranes with a polyethylene matrix. The reason is that, at 60 °C, the mechanical properties of the matrix polymers gradually deteriorate. The increase in matrix polymers elasticity allowed sulfonated PPS to expand more compared to a temperature of 35 °C. This resulted in the higher proton conductivity value. The polyethylene may be considered to deteriorate more rapidly than those of the remaining polymers under investigation. Since Amberlite is based on a cross-linked polymer backbone, its volume expansion during swelling by water is significantly lower compared to sulfonated PPS. Therefore, the temperature effect is not so pronounced here.

As expected, even the most conductive membranes do not reach the conductivity of the perfluorinated Nafion membrane in its fully swollen form. This is due to the lower content of the ion-conductive phase in the heterogeneous membranes compared to the homogeneous Nafion. The second aspect is the limited area of the contacts between the individual ion-exchanger particles inside the membranes, limiting to a certain degree, the charge and mass transfer in the heterogeneous membrane.

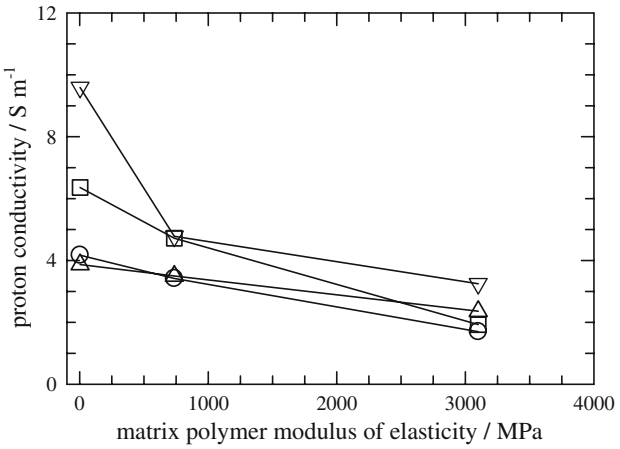

Fig. 9 Dependence of the heterogeneous membrane's proton conductivity on the modulus of elasticity of the matrix polymers for the individual ion-exchange resins used: *open circle* Amberlite at 35 °C, *open square* Amberlite at 60 °C, *open triangle* sulfonated PPS at 35 °C and *open inverted triangle* sulfonated PPS at 60 °C; modulus of elasticity of the individual matrix polymers studied: linear polyethylene (3 MPa), fluoroelastomer (736 MPa) and polystyrene (3,100 MPa). The concentration of ion-exchange particles in a dry membrane was always 66 wt%

3.2.4 *Proton diffusion coefficient*

The values of the proton diffusion coefficient obtained for the individual materials under study at 35 °C are summarised in Table 3. Its dependence on the modulus of elasticity of the matrix polymer is shown in Fig. 10. These data confirm the explanation of the proton conductivity dependence on the properties of the matrix polymer as well as of the ion-exchange resin provided above. The diffusivity of the proton

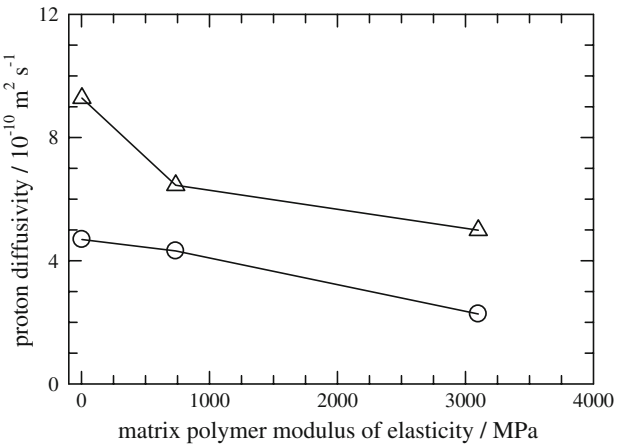

Fig. 10 Dependence of proton diffusion coefficient for membranes filled with *open circle* Amberlite and *open triangle* sulfonated PPS on the modulus of elasticity of the matrix polymers at 35 °C: linear polyethylene (3 MPa), fluoroelastomer (736 MPa) and polystyrene (3,100 MPa)

in the sulfonated PPS-based membranes is generally higher compared to the Amberlite-based samples. This is due to the non-crosslinked structure of this ion-exchange resin which thus has a larger free volume and consequently better proton transport properties. This explanation is further confirmed by the increase in the diffusivity value in the case of sulfonated PPS-based membranes with the polyethylene matrix. A significant diffusivity increase for this membrane is in agreement with the higher matrix flexibility accommodating more significant sulfonated PPS expansion and thus with a larger free volume inside the ion-exchanger phase.

The proton diffusivity value obtained corresponds quite well to the Nafion membrane representing a cross-linked material with a relatively rigid structure and to its degree of swelling in water.

3.2.5 Permeability to hydrogen and methanol

One important characteristic of a membrane to be used as a polymer electrolyte in a fuel cell technology is its permeability to hydrogen as a potential fuel. The results obtained for the membrane samples under study are summarised in Table 3. The highest permeability was observed for the polyethylene matrix membranes. This is in very good agreement with the theory of the most swollen membranes. It is possible to assume that hydrogen penetrates the membrane most efficiently through the void fraction, even when full of water, rather than through the compact polymer phase. The permeability was expected to decrease with the increasing modulus of elasticity. This is true for the membrane with the fluoroelastomer binder showing the lowest permeability value amongst the materials studied. During repeated experiments the membranes utilising rigid polystyrene as the matrix showed permeability to hydrogen two orders of magnitude higher. The reproducibility of the results was very poor. This clearly indicates that the reason for such behaviour is not the permeability of the membrane phase by itself, but the cracks in the membrane structure. Their origins can be identified mainly in the procedure of the membrane's removal from the protection foils after press-moulding and in the sample installation in the apparatus as discussed above. It is thus possible to consider the role of polymer matrix elasticity in the resulting membrane permeability as proven.

It is also interesting, from the point of view of the practical application, that the permeability to hydrogen of both the sulfonated PPS as well as the Amberlite-based membranes is lower than that of the Nafion membrane (except for the malfunctioning polystyrene binder). This can be mainly related to the low permeability of the polymer matrix to hydrogen. This results in an increased tortuosity factor of the membrane, thus leading to its lower permeability values. The prerequisite for such behaviour is the low void volume of the membrane. Another aspect is the membrane surface skin, formed mainly by the matrix polymer, thus reducing membrane cross-section active with respect to the hydrogen transport.

A similar explanation also applies in the case of membrane permeability to methanol. Methanol represents another fuel proposed for low temperature fuel cells. The main difference compared to hydrogen consists in the fact that, in the classical arrangement, methanol is applied to the fuel cell in the form of an acidic water solution. In contrast to the previous case of hydrogen permeability, the membrane is thus fully hydrated. Moreover, in the case of the membrane under current load, the polar molecule of methanol may be transported across the membrane in the solvatation shell of the proton. The experimental results obtained are summarised in Table 3. In the case of the Amberlite-based membranes no reliable permeability value was obtained for the fluoroelastomer matrix. This was because of an extremely high permeability value, indicating cracks in the samples. This is in agreement with the difficult synthesis of the membrane as discussed above.

In the case of the membrane under current load, the membrane's permeability to methanol substantially increased in all the cases under study. The increase was significantly more pronounced in the case of the sulfonated PPS-based membranes and the polyethylene matrix. This resulted from the higher ion-exchange capacity of this material compared to Amberlite. Second reason was the elasticity of polyethylene. Under these conditions it is possible to consider electroosmotic flux to be more significant under current load conditions. This corresponds to the number of methanol molecules transported across the membrane by the proton. The value of 0.32 obtained for the sulfonated PPS—polyethylene membrane is relatively close to the value of 0.53 obtained for the Nafion membrane. This indicates the significance of this mass transfer mechanism in this particular case.

4 Conclusions

Heterogeneous membranes were prepared by hot-moulding from the blends of ion-exchange particles and various inert polymers, differing, in particular, in their affinity to water and modulus of elasticity. The skin layer was formed on all the prepared membranes. The thickness of the skin layer and the membrane structure depended strongly on the matrix polymer and on the properties of ion-exchange particles. The most suitable structure was observed for a combination of Amberlite particles with polyethylene. This material shows sufficient interconnections between the individual ion-exchange particles, very thin skin layer sufficiently penetrated by the ion-exchange particles, and at

the same time, suitable mechanical properties. Similar structure was observed for the fluoroelastomer bound Amberlite. Its mechanical properties, however, were less promising than those of polyethylene. Sulfonated PPS particles have generally shown worse properties due probably to their size and noncrosslinked structure.

The characteristics of the heterogeneous membranes have proven the properties of the Amberlite—polyethylene membrane to be superior to those of the materials studied within this study. This is due to the suitable mechanical properties of both membrane phases and their compatibility. In selected cases, better conductivity may be obtained for the sulfonated PPS—polyethylene membrane. However, this material is significantly more permeable to hydrogen as well as to methanol.

The results of this study have demonstrated the important impact of the two heterogeneous membrane components on the characteristics of the resulting membrane. Not only the role of the ion-exchange phase, but also that of the matrix polymer is important. The information obtained provides a basic guide for the selection of the components to be used for the design of the heterogeneous ion-exchange membrane with the desired properties. Nevertheless, further intensive study is needed to provide deeper insight into the interactions between the matrix polymer and the ion-exchange phase of this type of materials.

Acknowledgements Financial support of this research provided by the Grant Agency of the Czech Republic (Grant No. 203/05/0080) and Ministry of Industry and Trade of the Czech Republic (No. 2A.1TP1/116) is appreciated.

References

1. Savadogo O (1998) J New Mater Electrochem Syst 1:47
2. Rikukawa M, Sanui K (2000) Prog Polym Sci 25:1463
3. Smitha B, Sridhar S, Khan AA (2005) J Membr Sci 259:10
4. Cropper MAJ, Geiger S, Jollie DM (2004) J Power Sources 131:41
5. Friedlander HZ (1968) In: Mark HF, Gaylord NG (eds) Encyclopedia of polymer science and technology, vol 8. Wiley, New York, p 633
6. Schauer J, Brožová L (2005) J Membr Sci 250:151
7. Vyas PV, Shah BG, Trivedi GS, Ray P, Adhikary SK, Rangarajan R (2001) J Membr Sci 187:39
8. Gohil GS, Shahi VK, Rangarajan R (2004) J Membr Sci 240:211
9. Chen S-L, Krishnan L, Srinivasan S, Benziger J, Bocarsly AB (2004) J Membr Sci 243:327
10. Shah BG, Shahi VK, Thampi SK, Rangarajan R, Ghosh PK (2005) Desalination 172:257
11. Chen N, Hong L (2002) Solid State Ionics 146:377
12. Gasa JV, Boob S, Weiss RA, Shaw MT (2006) J Membr Sci 269:177
13. Hu KY, Xu TW, Yang WH, Fu YX (2005) J Appl Polym Sci 98:494
14. Hu KY, Xu TW, Yang WH, Fu YX (2004) J Appl Polym Sci 91:167
15. Oren Y, Freger V, Linder C (2004) J Membr Sci 239:7
16. Zabolotsky VI, Nikonenko VV, Pismenskaya ND (1996) J Membr Sci 119:171
17. Volodina E, Pismenskaya N, Nikonenko V, Larchet C, Pourcelly G (2005) J Colloid Interface Sci 285:247
18. Bonnet B, Jones DJ, Roziere J, Tchicaya L, Alberti G, Casciola M, Massinelli L, Bauer B, Peraio A, Ramunni E (2000) J New Mater Electrochem Syst 3:87
19. Genova-Dimitrova P, Baradie B, Foscallo D, Poinsignon C, Sanchez JY (2001) J Membr Sci 185:59
20. Zaidi SMJ, Mikhailenko SD, Robertson GP, Guiver MD, Kaliaguine S (2000) J Membr Sci 173:17
21. Schauer J, Kůdela V, Richau K, Mohr R (2006) Desalination 200:632
22. Bouzek K, Cílová Z, Podubecká P, Paidar M, Schauer J (2006) Desalination 200:650
23. Millet P (1990) J Membr Sci 50:325
24. Ling J, Savadogo O (2004) J Electrochem Soc 151:A1604